



ISSN: 0976-3031

Available Online at <http://www.recentscientific.com>

CODEN: IJRSFP (USA)

*International Journal of Recent Scientific Research*  
Vol. 8, Issue, 11, pp. 21511-21516, November, 2017

**International Journal of  
Recent Scientific  
Research**

DOI: 10.24327/IJRSR

## Research Article

### EFFECT OF NONLINEAR SURFACE PROFILE OF SLIPPER BEARING ON ITS TRIBOLOGICAL PERFORMANCE

Sarma P K<sup>1</sup>., \*Ramakrishna Konijeti<sup>2</sup>., Subrahmanyam T<sup>3</sup>., Dharma Rao Vedula<sup>4</sup>.,  
Prasad L S V<sup>5</sup>., Sharma K V<sup>6</sup> and Ravi Kumar P<sup>7</sup>

<sup>1</sup>GITAM University, Visakhapatnam 530045, India

<sup>2</sup>K L University, Guntur 522502, India

<sup>3</sup>AU College of Engineering for Women, Visakhapatnam 530003, India

<sup>4</sup>GVP College of Engineering, Visakhapatnam 530048, India

<sup>5</sup>Andhra University, Visakhapatnam 530003, India

<sup>6</sup>JNTUH College of Engineering, Hyderabad 500085, India

<sup>7</sup>Miracle Institute of Technology, Visakhapatnam 535216, India

DOI: <http://dx.doi.org/10.24327/ijrsr.2017.0811.1087>

#### ARTICLE INFO

##### Article History:

Received 15<sup>th</sup> August, 2017

Received in revised form 25<sup>th</sup>  
September, 2017

Accepted 28<sup>th</sup> October, 2017

Published online 28<sup>th</sup> November, 2017

##### Key Words:

Slipper bearings, Nonlinear surfaces,  
Pressure distribution, Power transmission.

#### ABSTRACT

Tribology is the science and engineering of interacting surfaces in relative motion. It includes the study and application of the principles of friction, lubrication and wear.

**Objective:** The aim of this study is to develop a mathematical model to predict the variation of pressure between the slipper bearing surfaces when one of the surfaces is nonlinear.

**Methods:** The model evaluates the power requirement for transmission of a prescribed load for a given relative velocity between the nonlinear slipper bearing surfaces.

**Results:** A relative comparison between linear and nonlinear bearing surfaces is provided. The model results are in agreement with data from the literature. Further it has shown that the power transmission for nonlinear slipper bearings, depend on the profile index ( $n$ ) and Convergence ratio ( $\phi$ ).

**Conclusion:** A design criterion is put forward to specify the slipper surface for the reasonable power transmission.

**Copyright** © Sarma P K *et al*, 2017, this is an open-access article distributed under the terms of the Creative Commons Attribution License, which permits unrestricted use, distribution and reproduction in any medium, provided the original work is properly cited.

#### INTRODUCTION

A good analytical understanding of slipper behaviour in piston pumps and motors is crucial to good design. A large amount of work has been done in this area, but very little has focused on understanding the effect of nonlinear slipper surfaces. The general behaviour of a slipper will not drastically change because of nonlinearity, but their addition does modify the pressure distribution, and force acting over the slipper and this gives added design freedom.

Slippers have an important role on power dissipation in the swash plate axial piston pumps. The performance investigation of slipper designs is possible by a coupled numerical model of slipper lubrication (Andrew Schenk and Monika Ivantysynova, 2015). In order to calculate the slipper lubrication characteristics correctly, the film shape should be obtained precisely (Hong Liu *et al.*, 2011). A numerical model is

developed to predict the influence of film thickness and temperature on the slipper/swash plate interface under different operating conditions on slipper bearing carrying capacity (Hesheng Tang *et al.*, 2016). Experimental investigation on similar slipper bearings using different socket geometries, shown that socket geometry has a significant impact on the bearing performance (Noah D. Manring *et al.*, 2004).

For successful operation, the slippers need to have small amounts of non-flatness on the running surfaces (E. Koc and C. J. Hooke, 1997). The effects of non-flatness on the performance of slippers in axial piston pumps is analysed (C J Hooke and Y P Kakoullis, 1983). A new set of equations are developed (J.M. Bergada *et al.*, 2010), to evaluate the hydrostatic pressure distribution and lift on a grooved slipper having an ostensibly constant clearance. The motion and characteristics of slipper model of swash plate axial piston pumps and motors are discussed numerically under dynamic

\*Corresponding author: Ramakrishna Konijeti

K L University, Guntur 522502, India

conditions by focussing on the concave and convex geometries of the sliding surface (Toshiharu Kazama and Yukihito Narita, 2012).

The hydrodynamic performance characteristics of bearings can be analysed by evaluating pressure at various locations through grid refinement using FDM (Farooq Ahmad Najar and G. A. Harmain, 2014). A design criterion is proposed to specify the reasonable case drain pressure for a given slipper/swash plate pair within axial piston pump configuration (Bing Xu et al., 2015). A computational approach on the load carrying capacity of a slipper bearing is done to study the various parameters like the pressure, land area, conical angle of the land and the sleeper speed which has a direct relation on it (Kishan Choudhuri and Prasun Chakraborti, 2012).

The characteristic equation of hydrostatic slipper bearing is formulated for hydraulic axial piston motor (S. L. Nie et al., 2006) by considering the effects of the friction within the cylinder bore, the dynamics of the piston, and the centrifugal force of the piston-slipper assembly. Besides these, thixotropic behaviour of lubricants can have a dramatic effect on the pressure distribution under the slipper pad (K. Najmi et al., 2011).

The tribological characteristics of a complex tribomechanical system is analysed by using a simulation based numerical model (Sohil Hashemi et al., 2016) developed for calculation of multibody dynamics of slipper pad and piston incorporating a transient, 3D, thermal elasto hydrodynamic pivot pad contact with mixed lubrication configuration.

Surface texturing has been shown to be capable of enhancing the tribological contact performance for a wide range of applications. Introduction of controlled depressions and undulations on the surface of bearings can improve the tribological properties (Ulrika Pettersson and Staffan Jacobson, 2003). The evaluation of texture design by robust numerical models prior to being manufactured can avoid time consuming trial and error approaches (Daniel Gropper et al., 2016; T. Ibatan et al., 2015). Laser surface texturing (LST) is one of the most advanced surface texturing techniques in producing micro-dimple patterns for sliding contacts (L.M. Vilhena et al., 2009).

Artificial neural network (ANN) models are developed to determine the working parameters, the slipper geometry causing minimum frictional loss and to investigate the influence of the pattern, size and orientation of textures on slipper bearing load carrying capacity (Cem Sinanoglu, 2009; F. Canbulut et al., 2004). Niche genetic algorithm method is used to solve a unified model of slipper bearings in axial piston pumps and motors considering the interaction between tribological behaviour and dynamic performance (Shuo Lin and Jibin Hu, 2014), it outlined the effects of cylinder speed, loading pressure and oil viscosity on the behaviour of the slipper.

Most of these works are focused on analysing the pressure distribution, forces and torque for a specified slipper profile of linear, convex and concave. The method adopted for this analysis by the earlier researchers is cumbersome and or using a CFD package. Hence in this present work, a simple mathematical one-dimensional model is formulated to analyse

the pressure distribution in the lubricant due to nonlinear surface texture of the slipper and its effects on power transmission. The results obtained are compared with those available in the literature for similar profiles and are found in good agreement.

**Formulation**

The following assumptions are made in the analysis:

1. Film thickness is small compared with bearing dimensions.
2. The inertia of the lubricant is negligible.
3. The lubricant is unable to sustain sub-atmospheric pressure.
4. The lubricant is a simple Newtonian fluid with viscosity independent of shear rate.
5. Viscosity and density are constant throughout the bearing.
6. It is assumed that the bearing surfaces have high velocities, but the thickness of the film of lubricant is so small that the Reynolds number is usually far below its critical value for the system. i.e., Laminar flow occurs in the pressure-bearing film.

The configuration of the bearing surfaces is shown in Figure (1) with the load acting normal to the upper moving surface with a relative velocity  $u_{\infty}$ . The interspace between the bearing surfaces is separated by a lubricant with certain thermophysical properties. The pressure distribution is assumed to be unknown function of the space variable ( $X/L$ ) for the given geometric configuration of the surfaces.

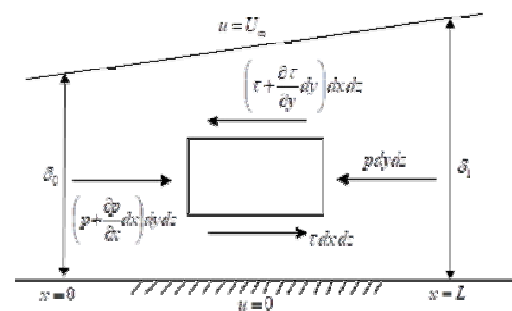


**Fig 1** Configuration of the bearing surfaces

The variation of the lubricant film thickness between the bearing surfaces is assumed as follows to account for non-linearity through the index n in the profile.

$$\frac{\delta}{\delta_0} = \left(\frac{X}{L}\right)^n (\phi - 1) + 1 \tag{1}$$

Where  $\phi = \left(\frac{\delta_1}{\delta_0}\right)$  and  $\tag{2}$

$$\delta = \delta_0 \text{ at } x = 0; \delta = \delta_1 \text{ at } x = L \tag{3}$$

The magnitude of index  $n = 1$  and  $\phi = 3$  are chosen for conventional slipper bearing surfaces. However, the present study includes the case for n with varying magnitudes physically representing non-linearity of the gap between the plates. Thus, the dynamics of flow of the lubricant between the

bearing surfaces can be defined by the following equations of motion for the coordinate system (x, y) shown in Figure 1.

$$\frac{\partial u}{\partial x} + \frac{\partial v}{\partial y} = 0 \tag{4}$$

Considering the equilibrium of forces and Newton's law of viscosity for the differential element

$$\frac{\partial^2 u}{\partial y^2} = -\frac{1}{\mu} \frac{\partial p}{\partial x} \tag{5}$$

The solution for Equation 5 is.

$$u = -\frac{1}{2\mu} \frac{\partial p}{\partial x} y^2 + C_1 y + C_2 \tag{6}$$

Equation 6 subject to the boundary conditions for the configuration shown in Figure 1 we get

$$y = 0 \Rightarrow u = 0; y = \delta \Rightarrow u = u_\infty \tag{7}$$

$$C_1 = \frac{u_\infty}{\delta} + \frac{1}{2\mu} \frac{dp}{dx} \delta \text{ and } C_2 = 0 \tag{8}$$

From Equation 6 and 8,

$$\therefore u = -\frac{1}{2\mu} \frac{dp}{dx} y^2 + \frac{y}{\delta} \left[ u_\infty + \frac{1}{2\mu} \frac{dp}{dx} \delta^2 \right] \tag{9}$$

Therefore, the flow rate of the lubricant in the film is

$$m = \rho \int_0^\delta u dy \tag{10}$$

Introducing Equation 9 in Equation 10

$$m = \left\{ \frac{\rho \delta^3}{12\mu} \frac{dP}{dx} + \frac{\rho u_\infty \delta}{2} \right\} \tag{11}$$

Equation 11 in dimensionless form can be written as

$$\frac{dP^+}{dX^+} = 12\pi_1 \frac{1}{(\delta^+)^3} - 6\pi_2 \frac{1}{(\delta^+)^2} \tag{12}$$

$$\Rightarrow \frac{dP^+}{dX^+} = 12\pi_2 \left[ \frac{Ratio}{(\delta^+)^3} - \frac{1}{2} \frac{1}{(\delta^+)^2} \right] \tag{13}$$

$$Ratio = \frac{\pi_1}{\pi_2} = \left[ \frac{m}{\rho \delta_0 u_\infty} \right] \tag{14}$$

$$\text{Where } \pi_1 = \frac{m \mu L}{\rho P_0 \delta_0^3}; \pi_2 = \frac{u_\infty \mu L}{P_0 \delta_0^2} \tag{15}$$

$$P^+ = \frac{P}{P_0}; X^+ = \frac{X}{L}; \delta^+ = \frac{\delta}{\delta_0} \tag{16}$$

$\pi_1$  - is dimensionless parameter associated flow rate of the lubricant in the clearance between the surfaces

$\pi_2$  - is the dimensionless parameter associated with the relative velocity of the bearing surfaces

Equation 1 in dimensionless form can be written as

$$\delta^+ = (X^+)^n (\phi - 1) + 1 \tag{17}$$

**Evaluation of  $\pi_1$  &  $\pi_2$**

Assume Tentatively, Ratio = 1

$$\text{i.e., } \pi_1 = \pi_2 \Rightarrow m = \rho \delta_0 u_\infty \tag{18}$$

where  $\delta = \delta_0$  at  $x = 0$

For the dynamic conditions of the lubricant at  $x=0$  and  $x=L$  and for the configuration of the non-linear bearing surfaces under consideration

$$P^+(X^+ = 0) = P^+(X^+ = 1) = 1 \tag{19}$$

Thus, the necessary geometric condition (18) to be preserved for the functioning of the bearing is as follows:

$$Ratio = \frac{\pi_1}{\pi_2} = \frac{1}{2} \left[ \int_0^1 \frac{dX^+}{[1+(X^+)^n(\phi-1)]^2} \right] \bigg/ \left[ \int_0^1 \frac{dX^+}{[1+(X^+)^n(\phi-1)]^3} \right] \tag{20}$$

Thus, for assumed values of  $\phi$  &  $n$ , The Eq. (21) can be evaluated to obtain the ratio i.e.,  $\pi_1 / \pi_2$

The above formulation implies that at the extreme boundaries of the bearing surfaces the pressures are one and the same as that of the value prevailing, at the ambience and the load bearing capacity of the bearing results in the generation of high pressures in the mid region of the bearing. Thus, the typical power estimation required to counter the load P at  $X^+=0.5$  can be estimated from the differential equation.

In the present study, a typical value of  $P^+ = 10$  at  $X^+ = 0.5$  is considered.

$$\frac{dP^+}{dX^+} = 12\pi_2 \left[ \frac{\pi_1}{\pi_2} \frac{1}{(\delta^+)^3} - \frac{1}{2} \frac{1}{(\delta^+)^2} \right] \tag{21}$$

Thus, the boundary conditions are as follows:

$$P^+ = 1 \text{ at } X^+ = 0; P^+ = P_c^+ \text{ at } X^+ = 0.5 \tag{22}$$

To satisfy boundary conditions (22) the magnitude of  $\pi_1$  can be numerically iterated for the differential equations (21). A typical graph is shown in figure (2).

**Evaluation of power**

$$\text{Power} = B P_0 L u_\infty \left[ \int_0^1 P^+ dx^+ \right] \tag{23}$$

$$\text{Where } u_{\infty} = \frac{\pi_2 P_0 \delta_0^2}{\mu L} \quad (24)$$

Equation 23 can be rearranged for dimensionless power as

$$\text{Dimensionless Power} = \frac{\text{power}}{BP_o L u_{\infty}} = \left[ \int_0^1 P^+ dX^+ \right] \quad (25)$$

Thus, the Power transmission for nonlinear slipper bearings depends on the profile index n, f as can be seen from Figures 5 & 6. Hence depending on the situation, it may be taken to advantage in the design through the choices of n and f. A generalized correlation in the estimation of power requirement is evaluated for wide range of parameters as follows applying regression analysis

$$2 < \phi \text{ (gap ratio)} < 4.5; 0.2 < n \text{ (Profile Index)} < 3; 12 < \pi_1 < 350; 45 < \pi_2 < 330; 4 < (P_c^+ \text{ at } X^+ = 0.5) < 12$$

$$\lambda = \left[ \frac{\text{power}}{BP_o L u_{\infty}} \right] = I = \int_0^1 P^+ dX^+ \\ = \pi_1^{0.1597} \pi_2^{-0.32} \phi^{0.202} n^{-0.1582} [P_c^+ \text{ at } X^+ = 0.5]^{1.137} \quad (26)$$

Equation 26 is validated in Figure 7 with the accuracy of Average deviation =2.3% and Standard deviation= 2.9%

## RESULTS AND DISCUSSION

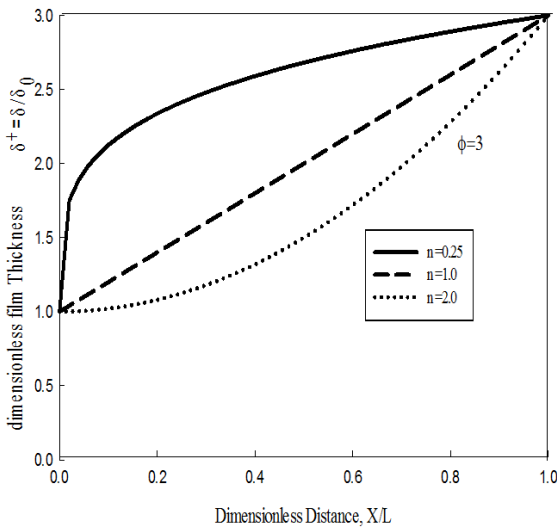


Figure 2 variation of Non-linear lubricant film thickness [Effect of profile index n]

Figure 2 shows the variation of film thickness in slipper bearing with different nonlinear profile indices. With increase in value of n the profile changes from convex to concave. For n=1 the thickness of lubricant film varies linearly in the bearing. It is observed from the Figure 2 that with increase in value of index of non-linearity the film thickness variation becomes more uniform.

Figure 3 shows the variation of pressure in the lubricant film along the length of the bearing. The distribution is shown for a profile index of n=2. The bearing pressure gradually increases reaches a maximum and again decreases. As predicted the maximum pressure point occurs approximately one-third distance from the beginning even though the point of

application of load is considered at the middle of the bearing due to clearance ratio greater than one.

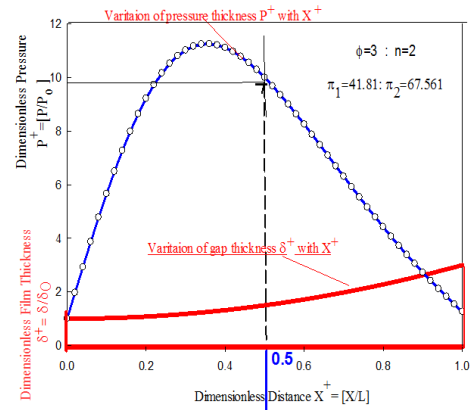


Figure 3 Typical Variation of Pressure in lubricant film for n=2 and P<sup>+</sup>=10 at X<sup>+</sup>=0.5

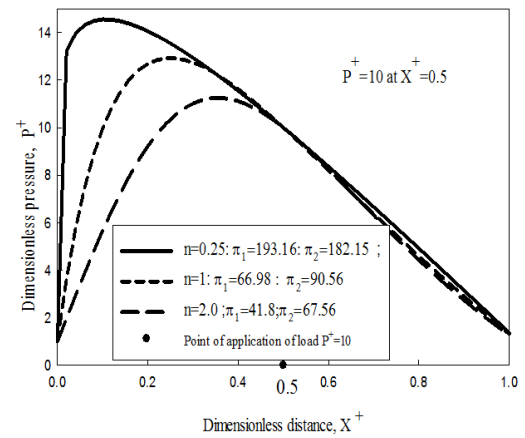


Figure 4 Variation of P<sup>+</sup> in the Lubricant for a Load application and P<sup>+</sup>= 10 at X<sup>+</sup>= 0.5

Further, with decrease in index the maximum pressure point shifts towards the lower clearance side as shown in Figure 4

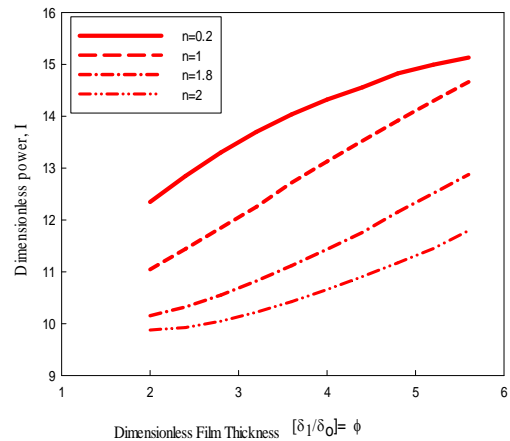


Figure 5 Variation of the power Rating with  $\phi$  [Effect of Profile Index of the Bearing]

For n=0.25 the peak pressure occurs almost at the entrance which represents more wear and tear at that point. Hence higher values of n are preferable as it leads to uniform variation of load along the length of the bearing.

Figure 5 shows the variation of power with increase in clearance ratio for different profile index values. With increase in clearance ratio the requirement of power increases.

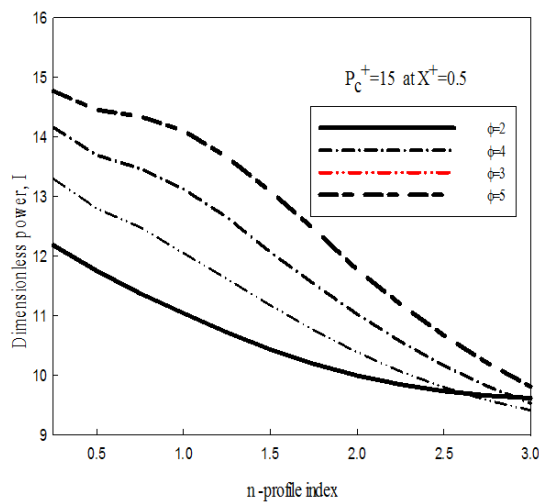


Figure 6 Effect of Profile Index n on Power for various Values  $\phi$

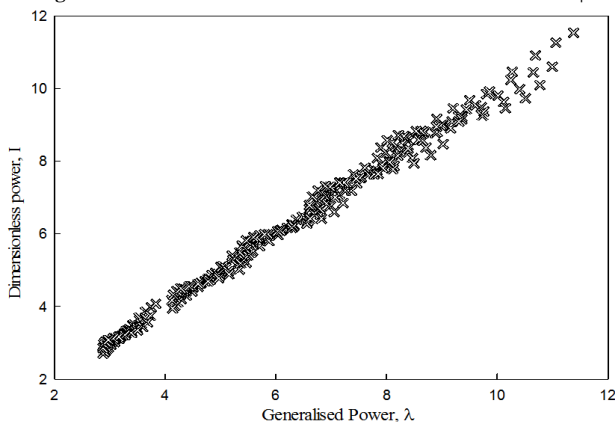


Figure 7 Validation of Equation 26

Figure 6 shows the variation of power with increase in index value for different Clearance ratio. With increase in index value the power rating decreases. Figure 7 validated the Equation 26 with the accuracy of Average deviation = 2.3% and standard deviation = 2.9%

## CONCLUSIONS

1. For clearance ratio one and linear profile the peak pressure occurs at the middle of the bearing. With increase in clearance ratio the maximum load point occurs towards less clearance side.
2. For a given clearance ratio with decrease in profile index the peak pressure point shifts more towards lower clearance.
3. The power requirement increases with increase in clearance ratio.
4. The power requirement decreases with decrease in profile index value n.

Thus, the power transmission for non-linear slipper bearings depends on the profile index n &  $\phi$  as can be seen from Figures 5, 6. Hence depending on the situation, it may be taken to advantage in the design through the choices of n &  $\phi$ .

## References

Andrew Schenk & Monika Ivantysynova, (2015). A Transient Thermoelasto hydro-dynamic Lubrication

Model for the Slipper/Swashplate in Axial Piston Machines, *J. of Tribology*, 137.

Hong Liu, Zengxiong Peng & Chujing Shen(2011). Film Shape Research of Slipper bearing in Axial Piston Pump Based on Genetic Algorithms, *Advanced Materials Research*, 302: 1533-1538.

Hesheng Tang, Yaobao Yin, & Jing Li (2016). Lubrication characteristics analysis of slipper bearing in axial piston pump considering thermal effect, *Lubrication science*, 28: 107-124.

Noah D. Manring, Chris L. Wray & Zhilin Dong(2004). Experimental Studies on the Performance of Slipper Bearings Within Axial-Piston Pumps, *J. of Tribology*, 126: 511-518.

E. Koc, & C. J. Hooke. (1997). Considerations in the design of partially hydrostatic slipper Bearings, *Tribology International*, 30(11): 815-823.

C J Hooke, & Y P Kakoullis,(1983). The effects of non-flatness on the performance of slippers in axial piston pumps, *Proceedings of the Institution of Mechanical Engineers*, 197C: 239-247.

J.M. Bergada, J.Watton, J.M. Haynes & D.L. Davies (2010). The hydrostatic/ hydrodynamic behavior of an axial piston pump slipper with multiple lands, *Meccanica*, 45:585-602.

Toshiharu Kazama & Yukihito Narita, (2012). Numerical Simulation of a Slipper Model for Swash Plate Type Axial Piston Pumps and Motors: Effects of Concave and Convex Surface Geometry, *Int. J. of Automation Technology*, 6(4):434-439.

Farooq Ahmad Najar & G. A. Harmain.(2014). Numerical Investigation of Pressure Profile in Hydrodynamic Lubrication Thrust Bearing, *International Scholarly Research Notices*, Article ID 157615

Bing XU, Qian-nan WANG & Jun-hui ZHANG(2015). Effect of case drain pressure on slipper/ swashplate pair within axial piston pump, *J. of Zhejiang University-SCIENCE A*, 16(12): 1001-1014.

Kishan Choudhuri & Prasun Chakraborti (2012). A Computational Approach on the Load Carrying Capacity of a Slipper Bearing, *Int. J. of Engineering and Technology*, 4(1): 52-56.

S.L. Nie, G.H. Huang & Y.P. Li.(2006). Tribological study on hydrostatic slipper bearing with annular orifice damper for water hydraulic axial piston motor, *Tribology International*, 39: 1342-1354.

K. Najmi, M. Karimzadeh & K. Sadeghy (2011). Lubricating flow of Thixotropic fluids in slipper- pad Bearing: A numerical study, *Journal of the Society of Rheology*, 39(4): 153-158.

Sohil Hashemi, Andreas Kroker, Lars Bobach, & Dirk Bartel(2016). Multibody dynamics of pivot slipper pad thrust bearing in axial piston machines incorporating thermal elasto-hydrodynamics and mixed lubrication model, *Tribology International*, 96

Ulrika Pettersson & Staffan Jacobson(2003). Influence of surface texture on boundary lubricated sliding contacts, *Tribology International*, 36 (11):857-864.

Daniel Gropper, Ling Wang & Terry J. Harvey(2016). Hydrodynamic lubrication of textured surfaces: A

- review of modeling techniques and key findings, *Tribology International*, 94
- T.Ibatan, M.S. Uddin, & M.A.K. Chowdhury (2015). Recent development on surface texturing in enhancing tribological performance of bearing sliders, *Surface and Coating technology*, 272:102-120.
- L.M. Vilhena, M. Sedlac̃ek, B. Podgorni, J. Viz̃intin, A. Babnik, & J. Moz̃ina,(2009). Surface texturing by pulsed Nd: YAG laser, *Tribology International*, 42: 496-1504.
- Cem Sinanoglu (2009). Investigation of load carriage capacity of journal bearings by surface texturing, *Industrial Lubrication and Tribology*, 61(5):261-270.
- F. Canbulut, S. Yildirim & C. Sinanog̃lu (2004). Design of an artificial neural network for analysis of frictional power loss of hydrostatic slipper bearings, *Tribology Letters*, 17(4):887-899.
- Shuo Lin & Jibin Hu (2014). Tribo-dynamic model of slipper bearings, *Applied Mathematical Modelling*, 39(2): 548-558.

**How to cite this article:**

Sarma P K et al.2017, Effect of Nonlinear Surface Profile of Slipper Bearing on Its Tribological Performance. *Int J Recent Sci Res.* 8(11), pp. 21511-21516. DOI: <http://dx.doi.org/10.24327/ijrsr.2017.0811.1087>

\*\*\*\*\*